

# Topology optimization of continuum structures with $\epsilon$ -relaxed stress constraints

C.E.M. Guilherme and J.S.O. Fonseca

*Federal University of Rio Grande do Sul, RS – Brazil*

## Abstract

Topology optimization of linear elastic continuum structures is a challenging problem when considering local stress constraints. The reasons are the singular behavior of the constraint with the density design variables, combined with the large number of constraints even for small finite element meshes. This work presents an alternative formulation for the  $\epsilon$ -relaxation technique, which provides an workaround for the singularity of the stress constraint. It also presents a new global stress constraint formulation. Derivation of the sensitivities for the constraint by the adjoint method is shown. Results for single and multiple load cases show the potential of the new formulation.

## 1 Introduction

Topology optimization is already established as an effective method for designing continuum mechanical structures. It has been developed to efficiently deal with strain energy based functions, as in its original application, compliance optimization. Relentless development has extended its usefulness; among many applications, it is nowadays used in compliant mechanisms, mechanical vibrations, wave propagation, and buckling [1, 2].

Most engineering situations, however, require the designs to pass pointwise failure criteria, usually based on the stress tensor. Thereby, topology optimization would greatly increase its usability if this kind of constraint could be successfully incorporated in its formulation.

Local constraints, however, are still a challenge to topology optimization. The large number of constraints in a discretized structure, combined with the inherently large number of design variables, conjure to create a large scale optimization problem. In the case of stress constraints, it is even more problematic; the finite element approximation of the stresses is naturally worse than displacements or energy, requiring finer meshes to achieve small errors.

The first tentatives to introduce failure criteria in topology optimization resorted to transform the local constraints into a single global constraint. These early attempts [3, 4] failed to achieve a fine control of the stresses in low density regions. Those shortcomings had already been noticed [5] in the

similar problem of truss layout optimization. In this field, this lack of convergence was associated with the singular behavior of the stress-area relation [6–8].

Cheng and Guo [9] developed a strategy to cope with stress singularity, a continuation approach called  $\epsilon$ -relaxation. In this case the stress constraint was relaxed by a expression containing a positive constant  $\epsilon$ ; when its value becomes zero the original stress constraint is recovered. The authors proposed a sequence of optimization problems which gradually reduces the value of the relaxation which would converge to the original constraint.

This idea was then adapted to continuum topology optimization with local stress constraints by [10]. Although they used an active set approach to reduce the number of simultaneous constraints, the computational cost of dealing with all the stress recovery points in the mesh was very high.

Fancello and Pereira [11, 12] introduced a new global stress constraint, which was combined with the  $\epsilon$ -relaxation technique to successfully reduce the computational cost of the optimization. Their works used an augmented Lagrangian formulation which lead to a box-constrained optimization, not very usual in topology optimization.

The  $\epsilon$ -relaxation is not without some critics, however; recent works [13] showed some cases where the continuation approach does not converge to the global optimal solution. Svanberg [14] indeed proposed a new approach based in a new discrete sensitivity analysis; but its results show that it is still not quite useful. Also the new phase-field approach [15] also has yet to be generalized to stress problems.

This work presents an alternative to formulate a multi-load case  $\epsilon$ -relaxed stress constrained topology optimization which can be solved by standard constrained mathematical programming methods. As the results show, this formulation shows a good potential to be easily coded into most topology optimization software.

## 2 Topology optimization

Topology optimization is defined as finding the material distribution inside a fixed domain  $\Omega$  so that an objective function is minimized, while a set of constraints are satisfied. The problem formulation starts by defining an artificial parametrized composite material, and obtaining a relation among these parameters and the constitutive properties. This work adopts a single parameter constitutive equation based on the density power law, with isotropic elastic properties, also called SIMP [1]:

$$E = \rho^r E^0 \quad (1)$$

where  $E$  is the composite's Young's modulus,  $\rho$  is the density,  $E^0$  is the base material Young's modulus, and  $r$  is the exponent of the power law, which behaves like a penalty factor. Thereby, the optimization is accomplished by finding the spatial distribution of the density.

As most structural analyses are performed with the finite element method, the density distribution is also defined with the finite element interpolation. In this case, it was chosen the usual constant density for each finite element. Thereby, the discretized optimization problem has as many design variables as the number of finite elements in the mesh.

## 2.1 Objective function

The natural choice for the objective function is the total mass of the design, in this case represented by

$$f(\rho) = \int_{\Omega} \rho \, d\Omega ; \quad (2)$$

but this work adopts a penalized version [16]

$$f(\rho) = \int_{\Omega} [\rho^q + \alpha\rho(1 - \rho)] \, d\Omega , \quad (3)$$

where  $q$  and  $\alpha$  are penalty coefficients, used to increase the relative cost of the intermediate densities.

Setting  $q = 1$  and  $\alpha = 0$  yields the volume of material; also ensures that the objective function is convex. It is usual to use a continuation approach by solving the problem with this objective function. Choosing  $0 < q \leq 1/p$  means that the cost of the intermediate densities increase faster than the elastic properties, so the optimization algorithm prefers to use either low or high densities. However the objective functions is non-convex; furthermore values close to zero cause ill conditioning to the problem. Choosing a coefficient  $\alpha < 0$  can mean that the intermediate density costs more than the base material, and is only used in the last part of the optimization to further clean the design from intermediate densities.

## 2.2 Checkerboard control

It is well known that the use of lower order finite element interpolation for the density can lead to some numerical instability, where the elemental densities may define a checkerboard pattern on low density areas. This phenomenon is usually avoided with the use of filtering, that is, some algorithm to constrain steep density variations. A move limit density filter [17] was implemented in this work.

## 3 Stress constraints

The main point of this work is present a new formulation for stress constraints. Sved and Ginos [5] first described convergence problems in truss optimization with stress constraints as some of the areas reached small values. They traced this instability to the stress singularity: as both forces and areas tended to zero, truss stress becomes undefined. Later works [6–8] stated that the optimum solution would be achieved with the removal of some of the bars, and suggested that a combinatorial method would be needed to test the many distinct layout possibilities. This problem was also noticed in the case of continuum topology optimization [3, 4].

The underlying idea of the  $\epsilon$ -relaxation [9] for truss optimization is to replace the stress constraint  $\sigma \leq \sigma_q$  by  $(\sigma - \sigma_q) A \leq \epsilon$ , where  $\epsilon$  is an arbitrary small number. As the problem converges, a new one is defined by reducing the value of  $\epsilon$ . A sequence of problems is solved until the relaxation reaches a previously defined threshold.

Although this method yields good results for truss optimization, its adaptation for the continuum case is not straightforward. Duysinx and Bendsøe [10] defined the relaxation for isotropic linear elasticity as

$$\rho \left( \frac{\sigma_{vM}}{\sigma_{lim}} - 1 \right) \leq \epsilon, \quad (4)$$

where  $\sigma_{vM}$  is the equivalent von Mises stress, and  $\sigma_{lim}$  the limit stress value. This equation was used as a local stress constraint, imposed in each finite element of the mesh. The large number of constraint equations is the main drawback of this approach.

The next step is the definition of a global stress constraint with relaxation. The well known alternatives are the  $p$ -norm [3]

$$\left\{ \int_{\Omega} \left( \frac{\sigma_{vM}}{\sigma_{lim}} \right)^p d\Omega \right\}^{\frac{1}{p}} \leq 1, \quad (5)$$

and the discrete Kreisselmeier-Steinhauser function [4]:

$$\frac{1}{p} \ln \sum_{i=1}^N e^{p \frac{\sigma_{vM}}{\sigma_{lim}}} \leq 1 \quad (6)$$

where  $N$  is the number of finite element stress points. Both approaches can emphasize the local stresses as the exponent increases; however, with a ill-conditioning as a side effect. Duysinx and Sigmund [18] modified the relaxation to

$$\begin{aligned} \rho \left( \frac{\sigma_{vM}}{\rho^n \sigma_{lim}} - 1 \right) &\leq \epsilon - \epsilon \rho \\ 1 &\geq \rho \geq \epsilon^2 \end{aligned} \quad (7)$$

and then introduced two different global stress constraints, the relaxed  $p$ -norm

$$\left\{ \sum_{e=1}^N \left[ \max \left( 0, \frac{\sigma_{vM,e}}{\rho_e^n \sigma_{lim}} + \epsilon - \frac{\epsilon}{\rho_e} \right) \right]^p \right\}^{\frac{1}{p}} \leq 1, \quad (8)$$

and the relaxed  $p$ -mean

$$\left\{ \frac{1}{N} \sum_{e=1}^N \left[ \max \left( 0, \frac{\sigma_{vM,e}}{\rho_e^n \sigma_{lim}} + \epsilon - \frac{\epsilon}{\rho_e} \right) \right]^p \right\}^{\frac{1}{p}} \leq 1, \quad (9)$$

where  $\sigma_{vM,e}$  is the von Mises equivalent stress for the finite element. The article cite some numerical difficulties to achieve convergence.

More successful was the work of Pereira et al. and Fancello and Pereira, [11, 12] which defined the global stress function as

$$\int_{\Omega} \max \left[ 0, \rho \left( \frac{\sigma_{vM}}{\sigma_{lim}} - 1 \right) - \epsilon + \rho \epsilon \right] d\Omega \leq 0 . \quad (10)$$

The problem is then solved by an augmented Lagrangian approach, which includes also a penalty for the norm of the density gradient. A box-constrained optimization mathematical programming algorithm was used.

In this work, after some testing with the existing relaxation expressions, an alternative  $\epsilon$ -relaxation is proposed,

$$\frac{\sigma_{vM}}{\sigma_{lim}} - 1 \leq \epsilon^{\rho} - \epsilon \quad (11)$$

which respects the original idea of Cheng and Guo: a continuous mapping from the perturbed problem to the original problem through the penalty  $\epsilon$ . This new relaxation is now used to define a global stress constraint based on the  $p$ -norm

$$\left\{ \sum_{e=1}^N \left[ \frac{v_e}{V_t} \max \left( 0, \frac{\sigma_{vM,e}}{\sigma_{lim}} + \epsilon^{\rho} - \epsilon \right) \right]^p \right\}^{\frac{1}{p}} \leq 1 , \quad (12)$$

where  $v_e$  is the element's volume and  $V_t$  the total domain volume. This additional fraction accounts for the possibility of unstructured meshes, where each element can have a different volume.

From the above expression it is evident that this constraint equality does not present a smooth behavior during the optimization iterations, as different elements might contribute to the constraint along the process.

#### 4 Sensitivity analysis

The expressions that define both the objective function and the global stress constraint can be analytically differentiated with respect to the discrete design variables. Therefore, mathematical programming algorithms can be easily implemented.

The objective function sensitivity is given by

$$f(\rho) = \int_{\Omega} [\rho^q + \alpha\rho(1 - \rho)] d\Omega , \quad (13)$$

which can be easily discretized and differentiated

$$f = \sum_{e=1}^N v_e [\rho_e^q + \alpha\rho_e(1 - \rho_e)] \Rightarrow \frac{\partial f}{\partial \rho_i} = v_i [q\rho_i^{q-1} + \alpha\rho_i(1 - 2\rho_i)] . \quad (14)$$

The proposed global stress constraint sensitivity derivation is somewhat more complex. Using the adjoint method, it can be written as

$$g(\sigma(\rho), \rho) = \left\{ \sum_{e=1}^N \left[ \frac{v_e}{V_t} \max \left( 0, \frac{\sigma_{vM,e}}{\sigma_{lim}} + \epsilon^{\rho_e} - \epsilon \right) \right]^p \right\}^{\frac{1}{p}}, \quad (15)$$

which is augmented with the equilibrium equation and an arbitrary multiplier vector  $\lambda$  as

$$h = g(\sigma(\rho), \rho) + \lambda^t (Ku - f) \quad (16)$$

which can be now differentiated with respect to a design variable  $\rho_e$ . Collecting the terms with the displacement sensitivity yields

$$\frac{dh}{d\rho_i} = \left( \frac{\partial g}{\partial \sigma_j} \frac{\partial \sigma_j}{\partial u} + \lambda^t K \right) \frac{\partial u}{\partial \rho_i} + \lambda^t \frac{\partial K}{\partial \rho_i} u + \frac{\partial g}{\partial \rho_i}. \quad (17)$$

Following the standard procedure, the term between parenthesis can vanish with the suitable choice of  $\lambda$  such that

$$\lambda = -K^{-1} \frac{\partial g}{\partial \sigma_j} \frac{\partial \sigma_j}{\partial u}, \quad (18)$$

remaining only

$$\frac{dh}{d\rho_i} = \lambda^t \frac{\partial K}{\partial \rho_i} u + \frac{\partial g}{\partial \rho_i}. \quad (19)$$

The derivatives in equation 18 can be developed by using the expression for the von Mises equivalent stress in the case of plane stress

$$\sigma_{vM} = \sqrt{\sigma_{11}^2 + \sigma_{22}^2 + 3\sigma_{12}^2 - \sigma_{11}\sigma_{22}} \quad (20)$$

$$= \sqrt{\begin{Bmatrix} \sigma_{11} \\ \sigma_{22} \\ \sigma_{12} \end{Bmatrix}^t \begin{bmatrix} 1 & -\frac{1}{2} & 0 \\ -\frac{1}{2} & 1 & 0 \\ 0 & 0 & 3 \end{bmatrix} \begin{Bmatrix} \sigma_{11} \\ \sigma_{22} \\ \sigma_{12} \end{Bmatrix}} \quad (21)$$

$$= \sqrt{\begin{Bmatrix} \sigma_{11} \\ \sigma_{22} \\ \sigma_{12} \end{Bmatrix}^t V \begin{Bmatrix} \sigma_{11} \\ \sigma_{22} \\ \sigma_{12} \end{Bmatrix}} \quad (22)$$

where the middle matrix is defined as  $V$ . For a specific element, the equation above can be written using the displacement-strain matrix  $B$  as

$$\sigma_{vM,i} = \sqrt{u^t \rho_i E^0 B^t V B \rho_i E^0 u} \quad (23)$$

$$= \sqrt{\rho_i^2 u^t E^0 B^t V B E^0 u} \quad (24)$$

so the needed derivative is expressed as

$$\frac{\partial \sigma_{vM,i}}{\partial u} = \frac{1}{2\sigma_{vM,i}} \frac{\partial}{\partial u} (\rho_i^2 u^t E^0 B^t V B E^0 u) \quad (25)$$

$$= \frac{1}{\sigma_{vM,i}} (\rho_i^2 E^0 B^t V B E^0 u) \quad (26)$$

The other term in equation 18 is given by

$$\frac{\partial g}{\partial \sigma_j} = \frac{\partial}{\partial \sigma_j} \left\{ \sum_{e=1}^N \left[ \frac{v_e}{V_t} \max \left( 0, \frac{\sigma_{vM,e}}{\sigma_{lim}} + \epsilon^{\rho_e} - \epsilon \right) \right]^p \right\}^{\frac{1}{p}} \quad (27)$$

which can be expanded as

$$\frac{\partial g}{\partial \sigma_j} = \left\{ \sum_{e=1}^N \left[ \frac{v_e}{V_t} \max \left( 0, \frac{\sigma_{vM,e}}{\sigma_{lim}} + \epsilon^{\rho_e} - \epsilon \right) \right]^p \right\}^{\frac{1-p}{p}} \left\{ \sum_{i=1}^N \left[ \frac{v_i}{V_t} \max \left( 0, \frac{\sigma_{vM,i}}{\sigma_{lim}} + \epsilon^{\rho_i} - \epsilon \right) \right]^{p-1} \right\} \frac{v_j}{V_t \sigma_{lim}} \quad (28)$$

Finally, the derivatives in equation 19 are

$$\frac{\partial g}{\partial \rho_i} = \left\{ \sum_{e=1}^N \left[ \frac{v_e}{V_t} \max \left( 0, \frac{\sigma_{vM,e}}{\sigma_{lim}} + \epsilon^{\rho_e} - \epsilon \right) \right]^p \right\}^{\frac{1-p}{p}} \left\{ \sum_{k=1}^N \left[ \frac{v_k}{V_t} \max \left( 0, \frac{\sigma_{vM,k}}{\sigma_{lim}} + \epsilon^{\rho_k} - \epsilon \right) \right]^{p-1} \epsilon^{\rho_i} \ln \epsilon \right\} \quad (29)$$

and

$$\frac{\partial K}{\partial \rho_i} u = L \frac{\partial K_i}{\partial \rho_i} u_i = L (q-1) \rho^{q-1} K_i^0 u_i, \quad (30)$$

where  $K_i^0$  is the element's stiffness matrix with the base material,  $L$  is the localization vector of the elemental displacements in the global displacement, and  $u_i$  is the elemental displacement vector.

The computational cost of the sensitivity analysis is not particularly high, since it requires only one additional matrix back-substitution for the adjoint problem given by equation 18 and a series of local elemental computations given by equations 28, 29, and 30.

## 5 Optimization procedure

The following optimization problem is formulated in this work: minimize the penalized function of the volume, subject to a von Mises stress constraint in each load case,

$$\begin{aligned} \min_{\rho} f &= \sum_{e=1}^N v_e [\rho_e^q + \alpha \rho_e (1 - \rho_e)] \\ g_l &\leq 0 \end{aligned} \quad (31)$$

where  $l$  spans the number of load cases.

A computer program for this formulation was written in C language, and the finite element code implemented the bilinear four-node plane stress element, with a single centroidal stress recovery point. The Sequential Linear Programming (SLP) algorithm with adaptive moving limits [17] was chosen for the optimization.

As mentioned before, the optimization procedure uses a continuation method, that is, a sequence of complete successive optimization problems. This means that each problem of the sequence must converge before the next starts, although for efficiency sake, the tolerance can be lowered in the early runs. The main path of this sequence is the reduction of the  $\epsilon$  relaxation factor; typically it starts with  $\epsilon = 0.5$  and reduces by 0.1 until it vanishes.

There are many coefficients to be reckoned in this formulation. The first one is the exponent of the constitutive power law, equation 1; all the results presented here used a simple linear scaling (law of mixtures). The other exponent is the power of stress norm, which for most cases was fixed as  $p = 4$ . The objective function defines its own continuation sequence; it starts linear ( $q = 1$ ,  $\alpha = 0$ ) while the  $\epsilon$  factor is changing, and then a sequence of optimization problems is solved by reducing the exponent  $q$  and increasing the coefficient  $\alpha$ . Typically, at the last run,  $q = 0.1$  and  $\alpha = 10$ .

Some remarks should be done after the test runs:

- As expected, global stress constraints with an active constraint set do not work with small meshes, because the constraint equation jumps noticeably at each design iteration.
- Moving limits filtering hampered convergence and had to be switched off. Reasons for this behavior are still under investigation.
- As noticed in [12], convergence for more than one load case is problematic, and depends on a fine tuning of the parameters.

## 6 Results

Results presented here use regular meshes. Limited testing with non-structured and three dimensional meshes did not yield any special difficulty, and is under thorough investigation.

The graphics show the resulting density plots, where black means full material, white means void. Gray areas represent intermediate densities. The underlying finite element mesh is noticeable, since the formulation uses constant density in each element.

### 6.1 Single load case

Two test cases are presented here; the first is a 1x3m rectangular domain supported by the upper edge under a unitary transverse load considering a material with  $E=21000\text{Pa}$ ,  $\nu = 0.3$ ,  $\sigma_{lim} = 35\text{Pa}$ .

As expected, the optimized design is a two-bar frame given by the following figure.

The second problem comes from [11]. It is the 1x1m L-shaped domain with 0.2m thickness supported at the top edge with a unitary vertical load in the middle of the lower vertical edge. The following values are used:  $E = 100\text{Pa}$ ;  $\nu = 0.3$ ;  $\sigma_{lim} = 42.42\text{Pa}$ . Notice that the equivalent stresses that violates the constraint are in the low density areas. The full material areas are respecting the constraint. Here it is possible to notice the formation of a smooth fillet, as expected.



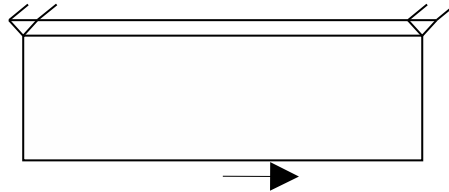


Figure 1: Rectangular design domain, support and loading

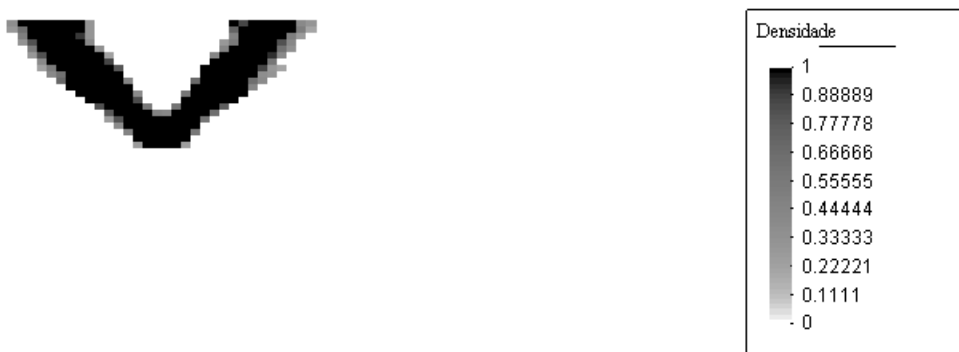


Figure 2: Optimized solution

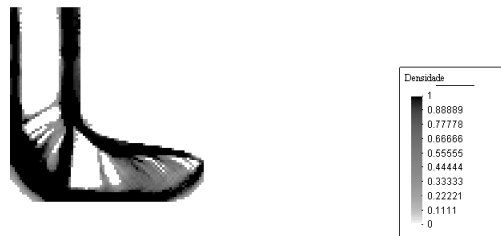


Figure 3: L-shaped optimal design

Comparing this results with [11], two main differences can be noticed: the lack of filtering causes small features in the designs presented here, and the penalized objective function means that the value of the objective function is also higher.

It is also interesting to address the concerns presented in [13]. From the practical point of view, it appears that a large number of design variables apparently mitigates the non-convergence issue.

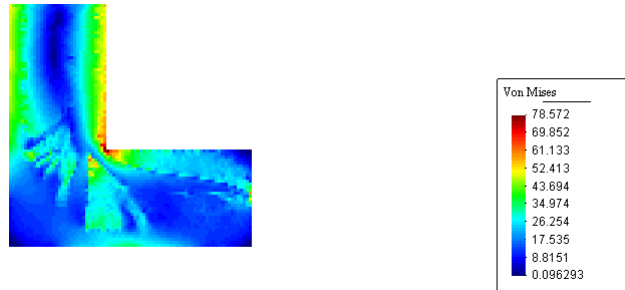


Figure 4: Equivalent stresses

## 6.2 Multiple load cases

The same L-shaped domain is now subject to a unitary horizontal load as the first load case and a unitary vertical load as the second load case.



Figure 5: L-shaped domain optimal design for two load cases

Results show the expected fillet; however it also presents a higher volume than the comparable work [12]; for instance there is no need to fill the lower left corner with material. This can also be attributed to the lack of filtering and excessive penalization of the objective function.

## 7 Conclusions

This work presents a formulation for the topology optimization of continuum structures subject to stress constraints for single or multiple load cases. The approach presented here lead to results comparable to existing literature. The results show that although the shortcomings of the  $\epsilon$ -relaxation

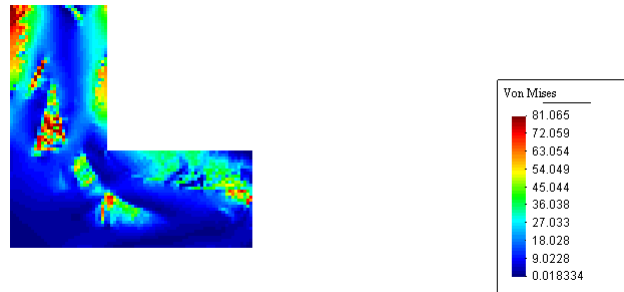


Figure 6: Stresses for the first load case

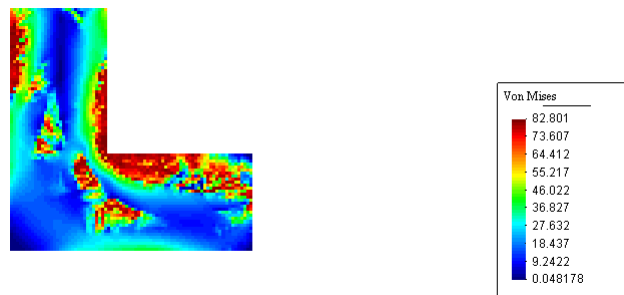


Figure 7: Stresses for the second load case

presented by Stolpe and Svanberg, it can be still be seen as a good heuristic method for stress constrained problems, at least until another formulation appears.

The main practical issues to be further developed in this formulation are the convergence issues with multiple load cases, test of other filtering algorithms, and an implementation with a faster optimization algorithm.

## References

- [1] Bendsøe, M. & Sigmund, O., *Topology Optimization - Theory, Methods and Applications*. Springer, 2003.
- [2] Bendsøe, M., Olhoff, N. & Sigmund, O., *IUTAM Symposium on Topological Design Optimization of Structures - Machines and Materials*. Springer, 2006.
- [3] Park, Y., Extension of optimal layout design using the homogenization method. *The U of Michigan Thesis*, 1995.
- [4] Yang, R. & Stress, C.C., Based topology optimization. *Structural Optimization*, **12**, pp. 98–105, 1996.
- [5] Sved, G. & Ginos, Z., Structural optimization under multiple loading. *Int J Mech Sci*, **10**, pp. 803–805, 1968.

- [6] Dobbs, M. & Felton, L., Optimization of truss geometry. *J Struct Div ASCE*, **95**, pp. 2105–2111, 1969.
- [7] Kirsch, U., On singular topologies of truss structures. *Structural Optimization*, **2**, pp. 133–142, 1990.
- [8] G.I.N. Rozvany, M.B.e. & Kirsch, U., Layout optimization of structures. *Applied Mechanics Reviews*, **48**, pp. 41–119, 1995.
- [9] Cheng, G. & Guo, X.,  $\epsilon$ -relaxed approach in structural topology optimization. *Eng Optimization*, **13**, pp. 258–266, 1997.
- [10] Duysinx, P. & Bendsoe, M., Topology optimization of continuum structures with local stress constraints. *Int J Numer Meth Engng*, **43**, pp. 1453–1478, 1998.
- [11] J.T. Pereira, E.F. & Barcellos, C., Topology optimization of continuum structures with material failure constraints. *Struc Multidisc Optimization*, **25**, pp. 1–17, 2003.
- [12] Fancello, E. & Pereira, J., Structural topology optimization considering material failure constraints and multiple load cases. *Latin American J Solids Struct*, **1**, pp. 3–24, 2003.
- [13] Stolpe, M. & Svanberg, K., On the trajectories of penalization methods for topology optimization. *Struct Multidisc Optim*, **21**, pp. 128–139, 2001.
- [14] Svanberg, K. & Werme, M., *Topology Design Optimization of Structures - Machines and Materials*, Springer, chapter Topology Optimization by Sequential Integer Programming, 2006.
- [15] Stainko, R. & Burger, M., *Topology Design Optimization of Structures - Machines and Materials*, Springer, chapter A One Shot Approach to Topology Optimization with Local Stress Constraints, 2006.
- [16] Haber, R., Bendsoe, M. & Jog, C., A new approach to variable topology shape design using a constraint on the perimeter. *Structural Optimization*, **11**, pp. 1–12, 1993.
- [17] Cardoso, E. & Fonseca, J., Complexity control in the topology optimization of continuum structures. *J Braz Soc Mechanical Sciences Engineering*, **25**, pp. 293–301, 2003.
- [18] Duysinx, P. & Sigmund, O., New developments in handling stress constraints in optimal material distribution. *7th Symp. in Multidisc. Analysis and Optimization*, AIAA/USAF/NASA/ISSMO, pp. 1501–1509, 1998.